2019/7/22

Reply to Reviewer 2

Manuscript title: Uncertainty caused by resistances in evapotranspiration

Dear Reviewer:

Thank you for carefully reading our manuscript and providing constructive suggestions and comments.
Below, we address all comments carefully point-by-point. All revisions are highlighted, i.e., newly added content is shown in blue, and any revised content is shown in red.
Our answers to every question/comment are provided below.

Reviewer: 2

The paper titled 'Uncertainty caused by resistances in evapotranspiration' by Zhao et al aimed at quantifying the uncertainties surface resistance parameterization to understand and improving terrestrial evapotranspiration (ET) models. This is a much-needed idea, however, the presentation of the manuscript needs substantial improvement before being published in HESS. Very surprisingly, the authors did not attempt to review the literatures carefully. It seems they are either not well versed with the recent literature that emphasized on overcoming the resistance estimation uncertainties. The empirical resistance model of Jarvis and KP has no physical basis. Here are my suggestions and comments, which needs to be considered before being approved for publications. I believe this manuscript can (and should) be improved substantially to give it good scientific quality.

Responses:

Thank you for appreciating our work and considering that the studied topic is a much-needed idea. We also thank you for pointing out the potential literature that we not included. Acknowledging this fact, we attempted to revise the manuscript with the help of your constructive comments and suggestions. With detailed replies to your comments, we believe that our manuscript has been improved substantially.

Comment 1:

Some recently published ET modeling and mapping studies that particularly addressed the challenges of resistance parameterizations (that deserves to be considered here); for example,

Mallick et al. (2018). Bridging Thermal Infrared Sensing and Physically Based Evapotranspiration Modeling: From Theoretical Implementation to Validation Across an Aridity Gradient in Australian Ecosystems, Water Resources Research, 54, 3409–3435. https://doi.org/10.1029/2017WR021357.

Mallick et al. (2015). Reintroducing radiometric surface temperature into the Penman-Monteith formulation, Water Resources Research, 51, 6214–6243, http://doi.org/10.1002/2014WR016106.

Garcia et al. (2013); Actual evapotranspiration in drylands derived from in-situ and satellite data: Assessing biophysical constraints. https://www.sciencedirect.com/science/article/abs/pii/S0034425712004828.

Morillas et al. (2013); Improving evapotranspiration estimates in Mediterranean drylands: The role of soil evaporation. https://agupubs.onlinelibrary.wiley.com/doi/pdf/10.1002/wrcr.20468.

Mallick et al. (2014). A surface temperature initiated closure (STIC) for surface energy balance fluxes, Remote Sensing of Environment, 141, 243 - 261.
Bhattarai et al. (2019). An automated multi-model evapotranspiration mapping framework using remote sensing and reanalysis data. Remote Sensing of Environment, 229, 69 - 92.
Gerhards et al. (2019). Challenges and Future Perspectives of Multi-/Hyperspectral Thermal Remote Sensing for Crop Water Stress Detection: A Review, Remote Sensing, 11(10), 1240; https://doi.org/10.3390/rs11101240.
Bhattarai et al (2018). Regional evapotranspiration from image-based implementation of the Surface Temperature Initiated Closure (STIC1.2) model and its validation across an aridity gradient in the conterminous United States, Hydrology and Earth System Sciences, 22, 2311-2341, https://doi.org/10.5194/hess-22-2311-2018.
Mallick, K., Trebs, I., Boegh, E., Giustarini, L., Schlerf, M., Drewry, D. T., et al. (2016). Canopy-scale biophysical controls of transpiration and evaporation in the Amazon Basin. Hydrology and Earth System Sciences, 20, 4237–4264. https://doi.org/10.5194/hess-20-4237-2016.
Katerji et al. (2011), Parameterizing canopy resistance using mechanistic and semiâA˘ Rempirical estimates of hourly evapotranspiration: critical evaluation for irrigated crops in the Mediterranean, https://onlinelibrary.wiley.com/doi/abs/10.1002/hyp.7829.

Responses:

Thank you for referring to these detailed publications.

In accordance with this comment, we added these publications within the appropriate sections (as well as citations in reference section) in this revised version. Some examples are as follows:

Although r_a can be difficult to determine because its calculation depends on certain parameters that are difficult to accurately obtain, such as the roughness height, zero-plane displacement, and atmospheric stratification (Brutsaert and Stricker, 1979; Gerhards et al., 2019), the uncertainty from r_a is often neglected.

Therefore, at low LAI (e.g., < 2), relatively high uncertainties were expected from single source models, such as those typically used in the PM equation (e.g., Farahani and Bausch, 1995; Lafleur and Rouse, 1990; Morillas et al., 2013).

However, surface or canopy resistances embody complex processes and are difficult to estimate accurately from RS data because they are controlled by numerous factors, such as wind speed (Su, 2002; Sánchez et al., 2008), vegetation type, biophysics, canopy architecture, soil texture and soil water availability (Leuning, 1995; Shuttleworth and Gurney, 1990; Katerji et al., 2011; García et al., 2013; Lehmann et al., 2018).

To avoid the issue of parameterizing resistances, several methods have been proposed to estimate ET without such parameterizations, such as the three-temperature (3T) model (Qiu et al., 2006; Xiong et al., 2015; Wang Y. et al., 2016), the surface temperature initiated closure model (Mallick et al., 2014, 2015, 2016, 2018; Bhattarai et al., 2018), the Priestley-Taylor method (Priestley and Taylor, 1972), the triangle or trapezoidal method (Price, 1990; Long and Singh, 2012), the complementary relationship model (Ma et al., 2019), and the surface renewal method (Paw U et al., 1995).

New references were also added (please note that Katerji et al. (2011) was in our previous manuscript):

Bhattarai, N., Mallick, K., Brunsell, N. A., Sun, G., and Jain, M.: Regional evapotranspiration from an

image-based implementation of the Surface Temperature Initiated Closure (STIC1. 2) model and its validation across an aridity gradient in the conterminous US, Hydrol. Earth Syst. Sci., 22, 2311–2341, https://doi.org/10.5194/hess-22-2311-2018, 2018.

Bhattarai, N., Mallick, K., Stuart, J., Vishwakarma, B. D., Niraula, R., Sen, S., and Jain, M.: An automated multi-model evapotranspiration mapping framework using remotely sensed and reanalysis data, Remote Sens. Environ., 229, 69–92, https://doi.org/10.1016/j.rse.2019.04.026, 2019.

García, M., Sandholt, I., Ceccato, P., Ridler, M., Mougin, E., Kergoat, L., Morillas, L., Timouk, F., Fensholt, R., and Domingo, F.: Actual evapotranspiration in drylands derived from in-situ and satellite data: Assessing biophysical constraints, Remote Sens. Environ., 131, 103–118, https://doi.org/10.1016/j.rse.2012.12.016, 2013.

Gerhards, M., Schlerf, M., Mallick, K., and Udelhoven, T.: Challenges and Future Perspectives of Multi-/Hyperspectral Thermal Infrared Remote Sensing for Crop Water-Stress Detection: A Review, Remote Sens., 11, 1240, https://doi.org/10.3390/rs11101240, 2019.

Mallick, K., Jarvis, A. J., Boegh, E., Fisher, J. B., Drewry, D. T., Tu, K. P., Hook, S. J., Hulley, G., Ardö, J., and Beringer, J.: A Surface Temperature Initiated Closure (STIC) for surface energy balance fluxes, Remote Sens. Environ., 141, 243–261, https://doi.org/10.1016/j.rse.2013.10.022, 2014.

Mallick, K., Boegh, E., Trebs, I., Alfieri, J. G., Kustas, W. P., Prueger, J. H., Niyogi, D., Das, N., Drewry, D. T., and Hoffmann, L.: Reintroducing radiometric surface temperature into the Penman-Monteith formulation, Water Resour. Res., 51, 6214–6243, https://doi.org/10.1002/2014wr016106, 2015.

Mallick, K., Trebs, I., Boegh, E., Giustarini, L., Schlerf, M., Drewry, D. T., Hoffmann, L., RANDOW, C. v., Kruijt, B., and Araùjo, A.: Canopy-scale biophysical controls of transpiration and evaporation in the Amazon Basin, Hydrol. Earth Syst. Sci., 20, 4237–4264, https://doi.org/10.5194/hess-20-4237-2016, 2016.

Mallick, K., Toivonen, E., Trebs, I., Boegh, E., Cleverly, J., Eamus, D., Koivusalo, H., Drewry, D., Arndt, S. K., and Griebel, A.: Bridging Thermal Infrared Sensing and Physically-Based Evapotranspiration Modeling: From Theoretical Implementation to Validation Across an Aridity Gradient in Australian Ecosystems, Water Resour. Res., 54, 3409–3435, https://doi.org/10.1029/2017wr021357, 2018.

Morillas, L., Leuning, R., Villagarcía, L., García, M., Serrano-Ortiz, P., and Domingo, F.: Improving evapotranspiration estimates in Mediterranean drylands: The role of soil evaporation, Water Resour. Res., 49, 6572–6586, https://doi.org/10.1002/wrcr.20468, 2013.

Comment 2:

Influence of the resistance parameterization on ET: Residual error analysis of ET with respect to resistance, soil moisture, VPD and net available energy (RN-G) needs to be discussed in detail.

Responses:

Thank you for the valuable comment.

In fact, we discussed the influence of the resistance parameterization on ET in Section 5.1 in our previous manuscript, although not in terms of residual error analysis used by Mallick et al. (Water Resources Research, 2018, 54, 3409–3435). Specifically, we discussed the influence of the resistance parameterizations under different physiological threshold value scenarios via the Jarvis model. We believe that, although the physical basis of the Jarvis model is not as perfect as that of other methods (such as

Medlyn et al. (2011) mentioned by reviewer 1), the inputs require certain types of physiological variables. Because measurements of such physiological variables are rare, we cited two values for a given physiological variable to perform the analysis, e.g., changing the minimum resistance, r_{smin}, from 20 to 150 s m^{-1} to investigate its impact on ET. In addition, these threshold values were carefully selected from the literature. Under such conditions, figure 10 could explain such a change in ET estimates.

In accordance with this comment, we analyzed the effects of r_s on ET under the one- and two-source PM equations in terms of the residual ET error. Figures 8 and 9 were added to the revision in combination with the corresponding context:

4.3 Sources of the differences among the LE estimates and model performance

Notably, the different LE estimates and model performance of the one-source PM equations were caused by the different resistance parameterizations (i.e., the difference between Eqs. (3) and (5) in Section 2.1). Figure 8a shows the large differences between r_s_JA, which was estimated in accordance with the methods of Jarvis (1976), and r_s_KP, which was estimated in accordance with the methods of Katerji and Perrier (1983). Specifically, if the r_s values greater than 1000 s m^{-1} in figure 8a are assumed to be outliers, the mean value of r_s_JA was 33 s m^{-1}, with maximum and minimum values of 705 and 9 s m^{-1}, respectively, whereas the mean value of r_s_KP was 300 s m^{-1}, with maximum and minimum values of 998 and 80 s m^{-1}, respectively. The average difference between the r_s_JA and r_s_KP estimates was 267 s m^{-1}, which led to a difference of 194 W m^{-2} in the LE estimates. Residual error analysis of LE (observation minus estimation) with respect to the r_s in figures 8b and 8c revealed that r_s_KP was generally underestimated, whereas r_s_JA was mostly overestimated (especially when r_s_JA < 200 s m^{-1}). Furthermore, quantification and parameterization of the surface resistance are difficult. For example, if the JA resistance method is applied at the residential site (No. 4 at 12:30 GMT+8 on July 10), the value of r_s is 288 s m^{-1}, leading to an LE value of 282 W m^{-2}, which was 107 W m^{-2} greater than the EC observation. Thus, the resistance estimation method and its parameterization can be major sources of uncertainty in ET estimates.

…

5 Discussion

5.1 Uncertainty caused by resistance in ET estimates

It is generally recognized that a complex model that can physically represent additional details of a system is more likely to give accurate estimations than a less complex model is. The results from the one-source PM equations support this idea. Because the results presented in Section 4 showed that the LE_JA values, which were estimated using the surface resistance parameterized from the physically based JA method, were more similar in terms of the MAPE to the observations than were the LE_KP values, which were estimated using the surface resistance parameterized from the empirical KP method. Nonetheless, compared to the variation in residual LE error versus r_s_JA (Figs. 8b and 8c), a relatively small variation in residual LE error versus r_s_KP indicates a stronger correlation between the LE_KP and observed LE values (R^2 = 0.9 in Fig. 4b). In addition, the complete one-source PM_JA method requires more parameters, such as the soil water and LAI (Tables S1 and S2), than does the PM_KP method, so LE cannot be estimated if a necessary variable is missing for a given time. This idea explains why the number of LE_KP estimates from the PM_KP method was greater than that from the PM_JA method (Fig. 4).

However, the relatively complex two-source PM equation performed more poorly than did the one-source PM equation, as shown in Section 4.2, which is likely due to the two-source PM equation requiring overcomplicated parameterizations. For example, the resistance parameterizations described by Mu et al. (2007) were improved in the report of Mu et al. (2011). In particular, the calculation of the surface resistance for vegetation involved different parameterizations of canopy conductance (g_c) (Table 3); the calculation of the surface resistance featured a r_{totc} value of 107 s m^{-1} (in Eq. 13); and the constant β in the soil-evaporation estimation was changed from 100 to 200 in the improved algorithm (Eq. 15). These modifications created different resistance values and LE estimates (abbreviated as LE_Mu_2007 and LE_Mu_2011) (Figs. 9a to 9c); however, these parameter changes are only locally optimized and might not generalize well. The LE values after the modifications were, on average, 104 W m^{-2} greater than those before the modification, and the root mean square error (RMSE) between LE_Mu_2007 and LE_Mu_2011 was 142 W m^{-2} (Fig. 9a). This difference was caused by the improvement in the resistance parameterizations. As shown in figures. 9b and 9c, the modification of the canopy conductance caused a difference of 39 s m^{-1} between the estimated canopy resistances, whereas the modification of r_{totc} produced a difference of 65 s m^{-1} in soil surface resistance. If the β value remained at 100 in the improved algorithm, the estimated LE values would have had an average difference of only 2 W m^{-2}. Therefore, the large difference (104 W m^{-2}) between the LE values before and after the modification was caused mainly by the differences in the resistance parameterizations. A weak relationship between the residual LE error and r_s values in figures. 9d to 9g further revealed that LE values estimated from the old but simple algorithms in the report by Mu et al. (2007) exhibited less bias (especially when $r_{s,\,c} < 400$ s m^{-1}) because estimation of g_c and r_{totc} became much more complicated in the improved algorithms, as shown in Table 3 (Mu et al., 2011). These results indicate that the uncertainty in ET estimation not only is caused by different resistance estimation methods but also can arise from the same method when using different parameterizations or assumptions (or nonunique parameterizations).

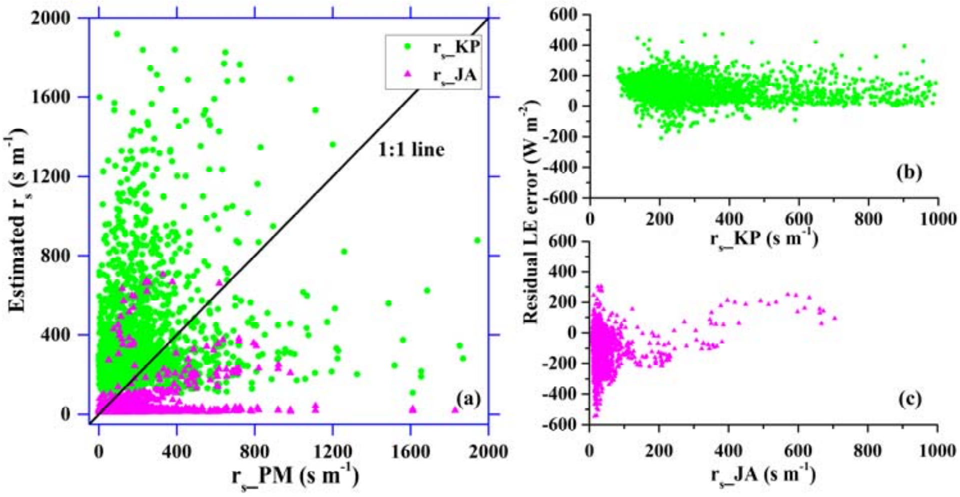

Figure 8: Differences in surface resistance, r_s (a), and scatter plots showing the effects of r_s on latent heat flux (LE) in terms of residual LE error (b and c).

Note: The LE values were estimated using the one-source PM equation and the same inputs except for r_s; r_s_JA, r_s_KP, and r_s_PM are r_s values from the method of Jarvis (1976), the method of Katerji and Perrier (1983), and the inverse of the one-source PM equation, respectively; residual LE error = difference between the observed LE and estimated LE.

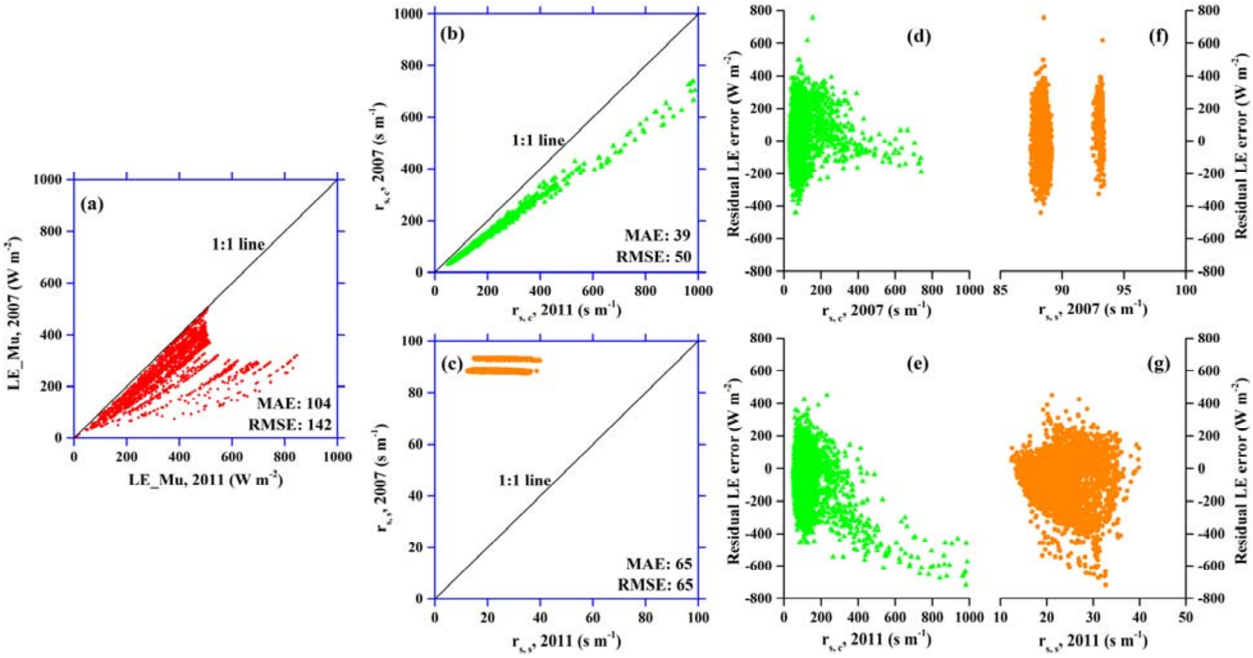

Figure 9: Differences in latent heat flux (LE) estimates from two versions of the PM_Mu algorithm (a) and resistances, $r_{s,c}$ (b) and $r_{s,s}$ (c); scatter plots showing the effects of $r_{s,c}$ ($r_{s,s}$) on LE in terms of residual LE error (d and e) (f and g).

Note: The LE values were estimated using the two-source PM equation; $r_{s,c}$ and $r_{s,s}$ represent the surface resistance of vegetation and the soil resistances, respectively; 2007 and 2011 refer to the old algorithms in the report of Mu et al. (2007) and the improved algorithms in the report of Mu et al. (2011); MAE and RMSE represent the mean absolute error and root mean squared error, respectively; residual LE error = difference between the observed LEs and estimated LEs.

Comment 3:

How the resistance models performed under different soil moisture, VPD and radiation conditions? Without a detailed analysis, it would be difficult to assess the scientific value of the paper.

Responses:

Thank you.

In fact, the performance of the different PM models at different maize sites was discussed in detail in figure 5 in the previous manuscript. The maize sites exhibited varied plant biophysics (LAI) and soil moisture contents (as well as VPD and net radiation). The results of the statistical analysis revealed that PM_KP performed better than did PM_JA in terms of R^2, with a mean value of 0.89 for the former compared with 0.73 for the latter. However, the MAPE values were generally greater than 30% for PM_KP and PM_JA. With respect to PM_Mu, R^2 was relatively low, with a mean value of 0.36, and the MAPE values were relatively large, with a mean value of 38.9%. Compared with the one-source PM equation, the two-source PM equation performed relatively poorly, which may likely be due to the two-source PM equation requiring over complicated parameterizations.

Because the first reviewer thought such statistical results of individual flux sites (in the previous figure 5) may not be meaningful for most readers who do not know the sites, we revised the figure by showing the model performance (MAPE) in the LAI-soil moisture space, attempting to provide intuitive information to readers in the event that they are not familiar with the sites (Fig. 6 as follows). There is no specific pattern in model performance in terms of LAI or soil moisture. In addition, the performance of the PM equation in this study was poor (MAPE > 30%); therefore, we believe it is unnecessary to perform a further analysis.

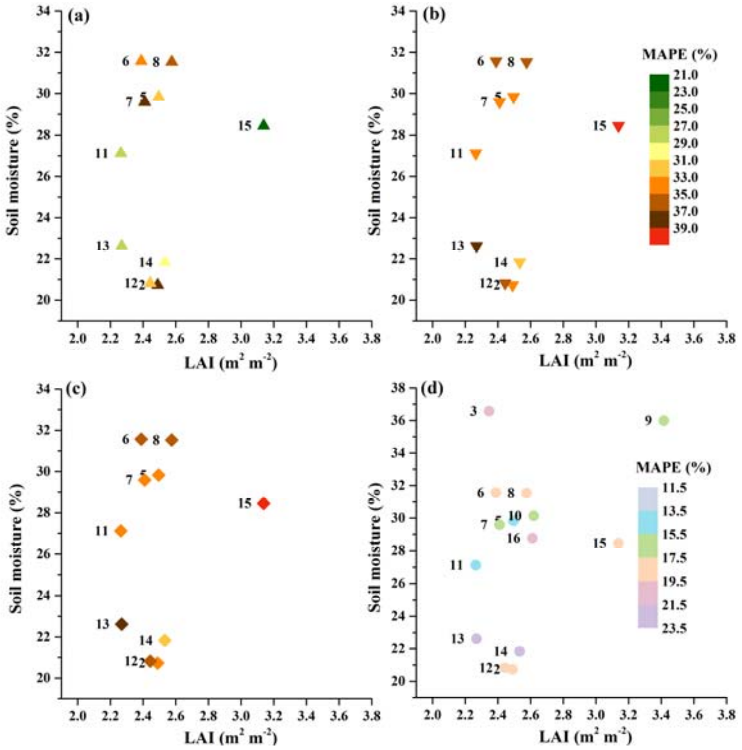

Figure 6: Performance of the different models at different maize sites under different leaf area index (LAI) and soil moisture conditions in terms of mean absolute percent error (MAPE): (a) PM_JA method, (b) PM_KP method, (c) PM_Mu method, and (d) the 3T model. Note: the number represents the EC system ID in figure 1c; the data are from figure 4; panels a, b, and c have the same color legend.

Comment 4:

How the 3T model performed under different soil moisture, VPD and radiation conditions?

Responses:

Thank you.

In fact, the performance of the 3T model at the different maize sites was discussed in detail in figure 5 of a previous manuscript. The maize sites exhibited varied plant biophysics (LAI) and soil moisture contents. The statistical results revealed that at the maize sites, the mean R^2 was 0.88 for the 3T model, with maximum and minimum values of 0.93 and 0.85, respectively; moreover, the MAPE values varied from 13.88% to 22.08%, with a mean value of 17.30%. Please see figure 4 in our reply to comment 3 for details. However, the performance of the 3T model also has no specific pattern. Its performance differed little only when the sites had similar (values close to each other) LAI and soil moisture content conditions, e.g., sites 2 and 12 and sites 5 and 7. For sites 2 and 5 (or 12 and 7), the LAI values were the same, but the MAPE value for site 5 with a relatively high soil moisture content was smaller than that of site 2 (or the model performed better at site 5). Nonetheless, with an even greater soil moisture content and similar LAI, site 3 was associated with the worst model performance among the three sites.

We also show the performance of the 3T model under different VPD and Rn conditions (Fig. R1 as follows). There is also no specific pattern of the model performance. Thus, it is unnecessary to add the results to the revised version.

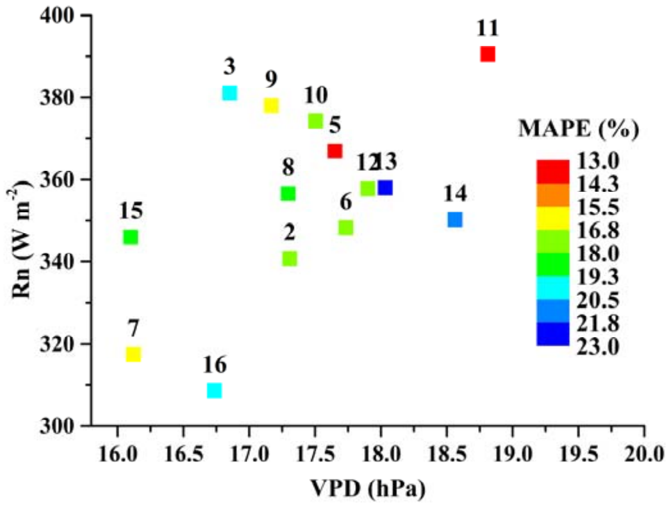

Figure R1: Performance of the 3T model at different maize sites under different VPD and Rn in terms of mean absolute percent error (MAPE). Note: the number represents the EC system ID.

In accordance with this comment, we added the abovementioned discussion to Section 4.2 in the revised version:

Generally, the 3T model performed much better than did both the one- and two-source PM equations; the MAPE was 19% for the 3T model, whereas it was greater than 32% for the PM equations. The one-source PM equation performed slightly better than that did the two-source PM_Mu. For the one-source method, the PM_JA caused the smallest biases in the LE estimation, whereas the empirical PM_KP model led to the largest uncertainty. Because the study area was a maize-dominated heterogeneous oasis and because the maize fields exhibited varied plant biophysics and soil moisture content conditions (Table 2), we further evaluated the model performance at different maize sites. The mean absolute differences in the LE values between the estimates and the observations were 105, 118, 131, and 60 W m^{-2} for PM_JA, PM_KP, PM_Mu, and the 3T model, respectively. Most of the MAPE values were greater than 30% for the PM equations, whereas they varied from 14% to 22% with a mean value of 19% for the 3T model (Fig. 6). Within the LAI-soil moisture space, the performance of the 3T model exhibited little difference only when flux sites had similar LAI and soil moisture content conditions (values close to each other), such as the values at sites 2 and 12 and sites 5 and 7. For sites 2 and 5 (or 12 and 7), the LAI values were the same, but the MAPE value for site 5 with a higher soil moisture was smaller than that of site 2 (i.e., the model performed better at site 5). Nonetheless, with an even greater soil moisture and similar LAI, site 3 associated with the worst model performance among the three sites. The performance of the 3T model under different VPD and Rn conditions was similar to that in the LAI-soil moisture space (results not shown here). The performance of the models varied for a given study site, with no specific pattern.

Comment 5:

A Table of symbols and their unit for different models would greatly improve the readability of the manuscript.

Responses:

Thank you.

We will add a table (Table A1) containing symbols and their units for the different models:

Table A1. Summary and description of variables and symbols

variables and symbols	units	description
ET	mm	evapotranspiration (evaporation + transpiration) as depth of water
E_c	mm	vegetation transpiration
E_s	mm	soil evaporation
L	J kg^{-1} K^{-1}	latent heat of vaporization
$L(ET)$	W m^{-2}	evapotranspiration (evaporation + transpiration) as latent heat flux
LE_c	W m^{-2}	vegetation transpiration as latent heat flux
LE_s	W m^{-2}	soil evaporation as latent heat flux
R_n	W m^{-2}	net radiation
$R_{n,s}$	W m^{-2}	net radiation of the soil component
$R_{n,c}$	W m^{-2}	net radiation of the vegetation component
R_s	W m^{-2}	solar radiation
G	W m^{-2}	soil heat flux
H	W m^{-2}	sensible heat flux
T_a	°C	air temperature
T_{0s}	°C	soil surface temperature
T_{0c}	°C	canopy temperature
T_L	°C	lower air temperature limits of stomatal activity method
T_{op}	°C	optimal air temperature limits of stomatal activity method
T_H	°C	upper air temperature limits of stomatal activity method
r_a	s m^{-1}	aerodynamic resistance
$r_{a,c}$	s m^{-1}	aerodynamic resistance for canopy
$r_{a,s}$	s m^{-1}	aerodynamic resistance for soil surface

r_s	s m^{-1}	surface resistance
r_{smin}	s m^{-1}	minimum stomatal resistance under optimal conditions
$r_{s,c}$	s m^{-1}	canopy resistance
$r_{s,s}$	s m^{-1}	soil surface resistance
g_s	m s^{-1}	leaf stomatal (surface) conductance
g_c	m s^{-1}	canopy conductance
γ	kPa $°C^{-1}$	psychrometric constant
VPD	kPa	vapor pressure deficit
Δ	–	slope of the saturation vapor pressure with respect to temperature
Rh	–	relative humidity
f_c	–	fractional vegetation cover
ρ_a	kg m^{-3}	mean air density at constant pressure
C_p	MJ kg^{-1} K^{-1}	specific heat of the air
z_r	m	reference height
z_{0m}	m	surface roughness length for momentum
z_{0h}	m	surface roughness length for heat
u_{zr}	m s^{-1}	wind speed at reference height
d	m	displacement height
θ	cm^3 cm^{-3}	soil water
θ_w	cm^3 cm^{-3}	wilting point
θ_f	cm^3 cm^{-3}	field capacity

Comment 6:

Analysis of Sensible heat fluxes should also be included in a condensed manner.

Responses:

Thank you.

In fact, we did not estimate the sensible heat flux (H). When estimating latent heat flux (LE) via residual methods of the energy-balance equation, H should be estimated first. However, in this study, we did not use a residual method of the energy-balance equation. We have H data from the tower observation, but we believe it may be strange to analyze H when discussing uncertainty in LE estimation without parameterizing H.

Comment 7:

How 3T model avoids the parameterization of the resistances? This is a good side of the model. However, it needs to be described in a condensed manner.

Responses:

Thank you.

We believe a clear description of the 3T model, such as nonparameterization of resistances, is necessary. Nonetheless, we have attempted to shorten the description while keeping key information:

2.3 The 3T model

The 3T model, which is derived from the energy balance equation, was first developed by Qiu (1996) and is loosely related to the three-leaf model of Paw U and Daughtry (1984). A unique characteristic of the 3T model is that the estimation of ET does not explicitly include any resistance parameterizations. A reference surface temperature (a dry surface without evaporation or transpiration) is used to eliminate latent heat and the surface resistance to water vapor under the assumption that the r_a for the reference soil is the same as that for other soil surfaces, resulting in Eq. (16) (see details in Qiu et al., 1996, 1998):

$$LE_s = R_{n,s} - G_s - \left(R_{n,sr} - G_{sr}\right)\frac{T_{0s} - T_a}{T_{0sr} - T_a} \qquad \text{soil} \qquad (16)$$

where T_{0s} in K is the temperature of the soil component; other variables are similar to previous ones, with subscripts "*s*" and "*sr*" indicating the soil component and the reference dry soil, respectively.

A similar technique was used to obtain Eq. (17) by introducing a reference dry vegetation surface:

$$LE_c = R_{n,c} - R_{n,cr}\frac{T_{0c} - T_a}{T_{0cr} - T_a} \qquad \text{vegetation} \qquad (17)$$

where T_{0c} is the temperature of the vegetation component and subscripts "*c*" and "*cr*" indicate the vegetation component and the reference dry canopy, respectively.

The total latent heat flux equation can then be calculated using Eq. (7). This unique feature makes the 3T model a relatively simple method for RS applications (Xiong & Qiu, 2011, 2014; Xiong et al., 2015; Wang Y. et al., 2016).